Available online at www.sciencedirect.com
ScienceDirect
Journal of Sound and Vibration 325 (2009) 69–84
JOURNAL OF SOUND AND VIBRATION
www.elsevier.com/locate/jsvi

Identification of crack in functionally graded material beams using the *p*-version of finite element method

Zhigang Yu[a,b], Fulei Chu[a,*]

[a]*Department of Precision Instruments and Mechanology, Tsinghua University, Beijing 100084, China*
[b]*Qinghe Building Ziba, Beijing 100085, China*

Received 8 May 2008; received in revised form 6 March 2009; accepted 10 March 2009
Handling Editor: L.G. Tham
Available online 16 April 2009

Abstract

The detection of cracks in functionally graded material (FGM) structural members has been a significant subject due to their increasing applications in various important engineering industries. A model-based approach is developed in this paper to determine the location and size of an open edge crack in an FGM beam. The *p*-version of finite element method is employed to estimate the transverse vibration characteristics of a cracked FGM beam. A rational approximation function of the stress intensity factor (SIF) with crack depth and material gradient as independent variables is presented in order to overcome the cumbersomeness and inaccurateness caused by the complicated expression of the analytical SIF solution in crack modeling. Subsequently the crack is represented by a massless rotational spring and its stiffness is obtained from fracture mechanics approach and the aforementioned SIF function. The proposed *p*-version finite element formulation and crack modeling are validated by analytical literature results of intact FGM beams and two-dimensional finite element analysis of cracked FGM beams with different supporting conditions and material gradients. The influences of crack size, crack location and material gradient on the natural frequencies of a cracked cantilever FGM beam are studied. To identify the crack parameters, the frequency contours with respect to crack location and size are plotted and the intersection of contours from different modes indicates the predicted crack location and size. Numerical experiments have demonstrated that the proposed method has excellent computational efficiency and satisfactory identification performance.

1. Introduction

In recent years functionally graded materials (FGM) have been regarded as one of the advanced inhomogeneous composite materials with great application potential in many high-temperature engineering fields such as aerospace vehicles, nuclear reactors, power generators, automobile industries. FGM are usually made from a continuous gradient mixture of metals and ceramics in compositional profile, hence they may take advantage of the heat and corrosion resistance of ceramics and the mechanical toughness of metals as well as reducing the magnitude of residual and thermal stresses. Cracks frequently occurred in FGM structures, which form a serious threat to their safe performance. Numerous research efforts have been

*Corresponding author.
E-mail address: chufl@mail.tsinghua.edu.cn (F. Chu).

0022-460X/$ - see front matter © 2009 Elsevier Ltd. All rights reserved.
doi:10.1016/j.jsv.2009.03.010

devoted on the fracture analysis of FGM with different configurations [1–4]. However, quantitative detection of the crack in FGM structures in advance is required for the application of these works in practice. Moreover, to prevent possible catastrophic failure when initial cracks grow to some critical level, early detection and prognosis of the damage is regarded to be rather valuable.

The presence of a crack in a structure will influence its stiffness, mass and damping properties and then change its vibration characteristics, which may be measured and employed to detect and quantify the crack. The vibration-based inspection approaches have received considerable attention in the last three decades. There are a large number of literatures that investigate crack modeling, free and forced vibrations and diagnosis of cracks. Chondros and Dimarogonas [5] provided a detailed overview of approaches to predict the change of dynamic characteristics versus crack location and size. Dimarogonas [6] reviewed the analytical, numerical and experimental studies on the recognition of cracks based on the changes in dynamic characteristics. Salawu [7] presented a survey of using natural frequency as a diagnostics parameter in the structural assessment procedures based on vibration monitoring. Doebling et al. [8] reviewed the methods of detection, localization and severity estimation of damages in the structural systems by examining changes in measured vibration responses.

According to the loading conditions and vibration amplitude, crack modeling usually fall into two categories: the open crack model and the breathing crack model [9]. In the opening crack model crack always opens during vibration while opens and closes alternately in the breathing model. The open crack model mainly includes an equivalent linear spring or local flexibility connecting the two segments of the beam, local change in the modulus of elasticity, reduced cross-sections and continuous flexibility variation along the length direction of the beam. A breathing crack, usually simulated by a bilinear spring, can produce interesting and complicated nonlinear dynamic behavior. Most of the previous research uses the open crack model whereas comparatively less studies have been carried out applying the breathing crack model. Rizos et al. [10] modeled the crack as the local flexibility and used a semi-analytical way to correlate the measured modes with the crack location and size. Narkis [11] simulated cracks as an equivalent rotational spring and studied the dynamics and identification problems of a cracked, simply supported uniform beam. Dado [12] reported a comprehensive crack identification algorithm for beams under different supporting conditions using the local flexibility approach. Christides and Barr [13] developed a one-dimensional continuous cracked Euler–Bernoulli beam theory through the generalized variational principle and an assumed crack disturbance function to be determined by experiments. Chondros [14] presented a continuous crack flexibility model based on fracture mechanics and validated this model by experimental results obtained on aluminum and steel beams with open cracks. Yang et al. [15] proposed a continuously varying bending stiffness expression of beams with an open crack based on energy method. Chondros et al. [9] used a bilinear crack model and the continuous cracked beam vibration theory to predict changes in transverse vibration of a simply supported beam with a breathing crack. It is worth noticing that these crack models must be properly applied with consideration of the assumptions under which the models were derived or valid, otherwise incorrect conclusions would be made.

The modal parameters used as damage indicators usually include natural frequency, mode shape or damping factor. Most of the literatures adopted natural frequency to identifying cracks [7]. The main reason for the popularity of natural frequency as a damage indicator is that they are rather easy to determine with a high degree of accuracy although they are not very sensitive to small crack. The quantitative crack identification methodology generally requires a mathematical model [16] that explicitly includes the crack size and location as model parameters and is capable of representing the key structural characteristics. The crack location and size estimation can be reached by comparing and minimizing the difference between the measured dynamic data and vibration results obtained from the structural model. A wide variety of methods have been presented to resolve these crack detection problems, which mainly consist of the classical or modern optimization approaches and the frequency contour method. Suh et al. [17] presented a hybrid neuro-genetic technique for identification from natural frequency results obtained from a finite element model of the cracked structure. Au et al. [18] used a micro-genetic algorithm to quantify the damage extent by minimizing the errors between the measured data and numerical results. These intelligent algorithms should be carefully used since the choice of parameters in these algorithms severely affects accuracy and efficiency of the crack identification. Additionally, considerable computational costs would be involved to generate numerical results to be

compared with the measured data so as to find the closest case in each of the crack identification processes. On the contrary, the frequency contour method can effectively overcome the foregoing drawbacks. In this method, the relation of structural natural frequency to the crack location and size is obtained based on the numerical model of a certain structure in advance. According to the given measured frequencies the frequency contour lines can be easily plotted. The intersection point of these superposed plots will indicate the crack location and size simultaneously. Owolabi et al. [19] used three frequency contour lines to estimate the normalized crack location and size of aluminum beams in an experimental study. Yang et al. [15] applied the approach to identify two cracks in a simply supported beam. Gounaris and Papadopoulos [20] employed the similar procedure to determine crack parameters in a rotating beam based on coupled response measurements.

Compared with the aforementioned extensive literature about investigation of cracked isotropic homogeneous beams and intact FGM structures [21–24], much less attention was focused on vibration and diagnosis of cracked FGM members. It is possibly due to the novelty of such materials and the complexity of crack modeling in FGM. Among the sparse works concerning to cracked FGM beam, Byrd and Birman [25] discussed closed-form solutions of the problems of free and forced vibrations of damaged FGM beam. Yang and Chen [26] employed the rotational spring model to represent a crack and a semi-analytical method to investigate free vibration and buckling characteristics of FGM beams with an edge crack. Later, Yang et al. [27] used the similar approach to study free and forced vibration of cracked FGM beam under an axial force and a moving load.

Finite element methods (FEM) have been widely to analyze cracked structures [28–30] since they can deal with engineering structures of complex geometry in a standard procedure. Most of them are based on the conventional finite element methods (CFEM). However, the convergence of CFEM depends on the number of elements used. To accurately acquire the higher-order mode, the element size should be very small to capture the corresponding high frequencies. Thus a large number of dof are required for accurately calculating the higher-order modes, which greatly increases the computational efforts. To overcome the shortcoming that CFEM has, the *p*-version of the FEM (*p*-FEM) was put forward for solving such problems [31]. The *p*-FEM has a few excellent features. The most important feature is that any desired degree of accuracy can be obtained by simply increasing the number of shape functions over the elements, while a fixed coarse mesh is used. The other important feature is that with respect to the number of dof, it offers more rapid convergence than the *h*-version of the FEM, which increases the accuracy by refining the mesh and is pervasively employed in CFEM. Hence, computational efforts can be saved by using the *p*-method.

The objective of this paper is to present an efficient methodology to estimate the crack location and size in FGM beams, which takes full advantages of the *p*-FEM in structural analysis. The *p*-version FGM beam element is constructed to analyze free vibration of cracked FGM beams and thus a more efficient identification can be obtained. The analysis is limited to open cracks just to avoid the nonlinearities associated with breathing crack models. The presence of cracks is assumed to only influence stiffness properties of the structure. Since the complicated analytical form of the stress intensity factor (SIF) in FGM beam under investigation is difficult to make use of in crack modeling, a convenient rational approximation function is applied to facilitate the calculation of local flexibility representing the effect of crack. The convergence and accuracy of the proposed method are examined by using the literature results of intact FGM beams and two-dimensional finite element analysis for cracked FGM beams. Subsequently the effects of crack location and size and material gradient on the natural frequencies are studied. Finally the frequency contours are obtained and employed to identify the crack in FGM beams. Numerical experiments are presented to demonstrate the effectiveness of the proposed procedure.

2. The *p*-FEM formulation for vibration analysis of a cracked FGM beam

Consider a FGM beam with an edge crack parallel to the direction of the material gradient undergoing transverse bending vibration, as shown in Fig. 1. In most of the existing solutions concerning FGM, material properties usually are assumed as either an exponential or a power function of a spatial variable. In the present study, the elastic modulus E, shear modulus μ and mass density ρ are taken to be of the following forms:

$$E(y) = E_0\, e^{\beta y}, \quad \mu(y) = \mu_0\, e^{\beta y}, \quad \rho(y) = \rho_0\, e^{\beta y}, \tag{1}$$

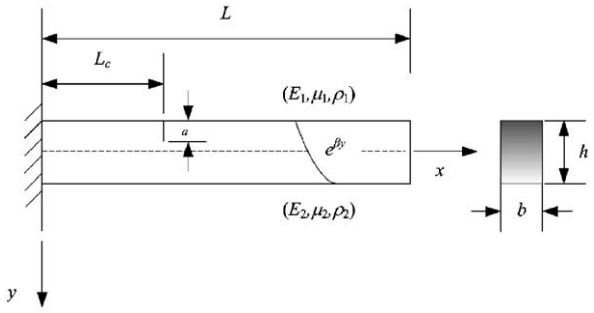

Fig. 1. A FGM beam with an open edge crack.

where E_0, μ_0, ρ_0 are the values of these elastic properties at $y=0$, $\beta=\ln(E_2/E_1)/h$ is a constant representing the material gradient. These forms of the material properties have been previously used by a number of investigators, e.g. Delale and Erdogan [32] and Noda and Jin [33].

The p-version FEM is adopted to model this cracked FGM beam. The beam is discretized into two intact FGM beam elements and a crack element from the crack section. The elements on the left and right sides of the crack are numbered as the first and second element, respectively. The constructions of the intact FGM beam elements and the crack modeling are presented below.

2.1. Governing equation of free vibration of intact FGM beams

According to Kirchoff–Love hypothesis, the axial displacement u can be expressed as

$$u(x,y,t)=-y\frac{\partial w(x,t)}{\partial x}, \tag{2}$$

where $w(x,t)$ denotes the transverse displacement of the beam. Using Eq. (2), the linear strain and stress in the x direction can be written as follows:

$$\varepsilon_x=\frac{\partial u}{\partial x}=-y\frac{\partial^2 w}{\partial x^2}, \quad \sigma_x=E(y)\varepsilon_x=-y\frac{\partial^2 w}{\partial x^2}E(y). \tag{3,4}$$

Then the strain energy S and kinetic energy T are given by

$$S=\frac{1}{2}\int_0^L\int_A \sigma_x\varepsilon_x\,\mathrm{d}A\,\mathrm{d}x, \quad T=\frac{1}{2}\int_0^L\int_A \rho(y)\dot{w}\,\mathrm{d}A\,\mathrm{d}x, \tag{5,6}$$

where $(\dot{\cdot})$ and A denote the differentiation with respect to time and the area of cross-section of the beam, respectively. Applying Hamilton's principle, the following differential equation of motion can be obtained:

$$D_{11}\frac{\mathrm{d}^4 w}{\mathrm{d}x^4}-I_1\frac{\mathrm{d}^2 w}{\mathrm{d}t^2}=0, \tag{7}$$

where $D_{11}=-b\int_{-h/2}^{h/2}y^2E(y)\,\mathrm{d}y$ and $I_1=-b\int_{-h/2}^{h/2}\rho(y)\,\mathrm{d}y$.

2.2. p-version FGM beam element for structural modal analysis

For simplicity and convenience in mathematical formulation, the local non-dimensional coordinate $\xi=2(x-x_i)/L_e-1$, where L_e is the element length and x_i the coordinate value of the left end of the element, is introduced.

The basic idea of the p-FEM is to use more terms of shape functions compared with that of CFEM to approximate the realistic deformation of a structure, thus achieving more rapid convergence than CFEM.

For a one-dimensional p-version FGM beam element, the transverse displacement w can be expressed as follows:

$$w = w_1\varphi_1 + \theta_1\varphi_2 + w_2\varphi_3 + \theta_2\varphi_4 + \sum_{i=5}^{n} w_i\varphi_i, \tag{8}$$

where w_1, θ_1, w_2 and θ_2 are the transverse displacements and slopes at the two end nodes of the beam element, w_i $(i>4)$ are generalized internal dof, φ_1 to φ_4 are the four standard Hermite cubics, φ_i $(i>4)$ are higher-order interpolating functions which possess C^1 continuity and form a complete set. Here the shifted Legendre polynomials are adopted since they are second derivative orthogonal with respect not only to themselves but also to the first four Hermite cubics. Furthermore, they contribute a value of zero at each end of the element, hence not affecting the imposition of boundary conditions through nodal constraints alone. These functions have the following expressions:

$$\varphi_i(\xi) = \sum_{k=0}^{[(i-1)/2]} \frac{(-1)^k(2i-2k-7)!!}{2^k k!(i-2k-1)!}\xi^{i-2k-1}, \quad i>4, \tag{9}$$

where $k!! = k(k-2)\cdots 2$ or 1, $0!! = (-1)!! = 1$ and $[\cdot]$ denotes taking integer part.

The shape functions in Eq. (8) can be written in row matrix form as

$$\mathbf{N} = [\varphi_1 \ \ \varphi_2 \ \ \varphi_3 \ \ \varphi_4 \ \ \varphi_5 \ \ \cdots \ \ \ \varphi_n]. \tag{10}$$

After constructing the higher-order shape functions, the stiffness matrix and the mass matrix are obtained according to Eq. (7) and the standard procedure of the Galerkin FEM. The stiffness and mass matrices are represented in terms of the local coordinates as

$$\mathbf{K}_e = \frac{8D_{11}}{L_e^3}\int_{-1}^{1} \frac{\mathrm{d}^2\mathbf{N}^{\mathrm{T}}}{\mathrm{d}\xi^2}\frac{\mathrm{d}^2\mathbf{N}}{\mathrm{d}\xi^2}\,\mathrm{d}\xi, \quad \mathbf{M}_{\mathrm{e}} = \frac{I_1L_e}{2}\int_{-1}^{1}\mathbf{N}^{\mathrm{T}}\mathbf{N}\,\mathrm{d}x. \tag{11,12}$$

Substituting Eq. (10) into Eqs. (11) and (12), one can acquire the explicit forms of the element stiffness and mass matrices by symbolic computations. As an illustration, when $n = 8$ the expressions of the two matrices are given as follows:

$$\mathbf{K}_e = \frac{D_{11}}{L_e^3}\begin{bmatrix} 12 & 6L_e & -12 & 6L_e & 0 & 0 & 0 & 0 \\ & 4L_e^2 & -6L_e & 2L_e & 0 & 0 & 0 & 0 \\ & & 12 & -6L_e & 0 & 0 & 0 & 0 \\ & & & 4L_e^2 & 0 & 0 & 0 & 0 \\ & & & & \frac{16}{5} & 0 & 0 & 0 \\ & Sym & & & & \frac{16}{7} & 0 & 0 \\ & & & & & & \frac{16}{9} & 0 \\ & & & & & & & \frac{16}{11} \end{bmatrix},$$

$$\mathbf{M}_e = \frac{I_1 L_e}{420}\begin{bmatrix} 156 & 22L_e & 54 & -13L_e & 14 & \frac{-8}{3} & 0 & \frac{2}{33} \\ & 4L_e^2 & 13L_e & -3L_e & 3L & \frac{-L_e}{3} & \frac{-L_e}{9} & \frac{L_e}{33} \\ & & 156 & -22L_e & 14 & \frac{8}{3} & 0 & \frac{-2}{33} \\ & & & 4L_e^2 & -3L_e & \frac{-L_e}{3} & \frac{L_e}{9} & \frac{L_e}{33} \\ & Sym & & & \frac{8}{3} & 0 & \frac{-16}{99} & 0 \\ & & & & & \frac{8}{33} & 0 & \frac{-16}{429} \\ & & & & & & \frac{8}{143} & 0 \\ & & & & & & & \frac{8}{429} \end{bmatrix}.$$

2.3. Crack modeling

In order to study the effect of the crack on the dynamic behavior of the FGM beam, the crack model has to be established firstly. Based on fracture mechanics principles, the additional strain energy produced by the crack for plane stress [34] is

$$U_c = b\int_0^a \frac{K_{\mathrm{I}}^2}{E(y)}\,\mathrm{d}a, \tag{13}$$

where K_{I} is the SIF under the mode-I loading condition and is a function of the beam geometry, the external loading and the material properties. For a FGM strip with an open edge crack subject to bending illustrated in Fig. 1, the analytical solution of the SIF was given by Erdogan and Wu [4] as

$$K_{\mathrm{I}} = -\frac{4\mu(a)\sqrt{a}}{1+\kappa}\sum_{n=0}^{\infty} A_n, \tag{14}$$

where $\mu = E/2(1+v)$ is the shear modulus with v being the Poisson's ratio, $\kappa = 3-4v$ for plain strain and $\kappa = (3-v)/(1+v)$ for plain stress, A_n are to be determined through calculating the boundary integrals using Gaussian quadrature approach and then solving the resulting functional by collocation method. It can be seen that the form of K_{I} contains infinite terms, which is quite inconvenient in practical calculation. To overcome this drawback, we express the SIF in the common form used in isotropic homogeneous materials as follows [35]:

$$K_{\mathrm{I}} = \sigma_0\sqrt{\pi a}F(E_2/E_1, a/h), \tag{15}$$

where $\sigma_0 = 6M/bh^2$ with M being the external bending and F is an unknown function of two independent variables. Through a number of numerical experiments, the function F is eventually determined to be expressed as a rational function:

$$F(E_2/E_1, a/h) = \frac{p_1 + p_2\ln(E_2/E_1) + p_3[\ln(E_2/E_1)]^2 + p_4[\ln(E_2/E_1)]^3 + p_5(a/h) + p_6(a/h)^2}{1 + p_7\ln(E_2/E_1) + p_8[\ln(E_2/E_1)]^2 + p_9(a/h + p_{10}(a/h)^2 + p_{11}(a/h)^3}, \tag{16}$$

where the coefficients $p_1, p_2, \ldots, p_{11} = 1.1732, -0.3539, 0.0289, -0.0061, 0.6625, 3.0720, -0.0014, -0.0017, 1.9917, -0.3496$ and -3.0982 are determined by fitting Eq. (15) based on the least square method to the numerical values of the SIF for specific material gradients and normalized crack size given by Erdogan and

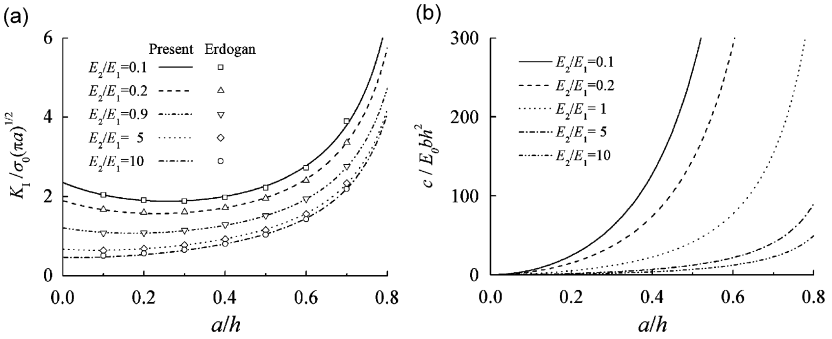

Fig. 2. (a) Stress intensity factor in FGM and (b) computed local flexibility.

Wu. The numerical values of the SIF and the resulting approximation are plotted in Fig. 2(a) and excellent agreement can be observed.

From Castigliano's theorem [36], the additional local flexibility due to the crack is

$$c = \frac{\partial^2 U_c}{\partial M^2}. \tag{17}$$

Using Eqs. (13), (15)–(17), one can compute the local flexibility. The computed results for several material gradients are shown in Fig. 2(b). Here the effects of the crack are simulated by a massless rotational spring. The spring connects the adjacent left and right elements and couples the slopes of the two FGM beam elements at the crack location. Based on the stiffness matrices of the two FGM beam elements and the open crack model, the global stiffness matrix of the cracked FGM beam can be assembled as follows:

$$\mathbf{K} = \begin{bmatrix}
K^1_{1,1} & K^1_{1,2} & K^1_{1,3} & K^1_{1,4} & 0 & 0 & 0 & & & & & & & \\
K^1_{2,1} & K^1_{2,2} & K^1_{2,3} & K^1_{2,4} & 0 & 0 & 0 & & & & & & & \\
K^1_{3,1} & K^1_{3,2} & (K^1_{3,3}+K^2_{1,1}) & K^1_{3,4} & K^2_{1,2} & K^2_{1,3} & K^2_{1,4} & & & & & & & \\
K^1_{4,1} & K^1_{4,2} & K^1_{4,3} & \left(K^1_{4,4}+\frac{1}{c}\right) & -\frac{1}{c} & 0 & 0 & & & & & & & \\
0 & 0 & K^2_{2,1} & -\frac{1}{c} & \left(K^2_{2,2}+\frac{1}{c}\right) & K^2_{2,3} & K^2_{2,4} & & & & & & & \\
0 & 0 & K^2_{3,1} & 0 & K^2_{3,2} & K^2_{3,3} & K^2_{3,4} & & & & & & & \\
0 & 0 & K^2_{4,1} & 0 & K^2_{4,2} & K^2_{4,3} & K^2_{4,4} & & & & & & & \\
 & & & & & & & K^1_{5,5} & 0 & \cdots & 0 & & & \\
 & & & & & & & 0 & K^1_{6,6} & \cdots & 0 & & & \\
 & & & & & & & \vdots & \vdots & \ddots & \vdots & & & \\
 & & & & & & & 0 & 0 & \cdots & K^1_{n,n} & & & \\
 & & & & & & & & & & & k^2_{5,5} & 0 & \cdots & 0 \\
 & & & & & & & & & & & 0 & K^2_{6,6} & \cdots & 0 \\
 & & & & & & & & & & & \vdots & \vdots & \ddots & \vdots \\
 & & & & & & & & & & & 0 & 0 & \cdots & K^2_{n,n}
\end{bmatrix} \tag{18}$$

where $K^k_{i,j}$ denotes the component at the ith row and jth column of the kth element stiffness matirx. The upper submatrix and the other two submatrices in Eq. (18) correspond to the standard cubic and the higher-term of shape functions, respectively. The order of the global stiffness matrix $\mathbf{K}$ is $2n-1$.

2.4. Finite element equations for free vibration

By using the standard procedures of traditional FEM, the eigenvalue problem can be obtained as

$$(\mathbf{K} - \omega^2\mathbf{M})\mathbf{W} = 0, \tag{19}$$

where $\mathbf{K}$ and $\mathbf{M}$ are the global stiffness and mass matrices, $\mathbf{W}$ is the column vector of the amplitudes of the nodal displacements, ω is the natural frequency of vibration. The solution of the eigenvalue problem can then proceed as usual.

3. Validation of the proposed method

In order to verify the applicability and performance of the present formulation, comparisons of the present method with the available data in the literature and two-dimensional FEM models are made. Unless otherwise stated, the FGM beam under investigation has the following material and physical parameters: $E_1 = 70\,\text{GPa}$, $\rho_1 = 2780\,\text{kg/m}^3$ at the top surface and slenderness ratio $L/h = 20$, normalized crack size $a/h = 0.2$. Different material gradient and supporting conditions are considered.

The first case study concerns free vibration of an intact FGM beam. The lowest three modal frequencies of the FGM beam with cantilever and clamped–clamped boundary conditions are calculated by the present p-FEM and the CFEM, respectively. The results as well as the solutions given by Yang et al. [26], which are all

Table 1
Comparison of the first three non-dimensional natural frequencies of intact FGM beams.

Method	$E_2/E_1 = 0.2$			$E_2/E_1 = 1$			$E_2/E_1 = 5$		
	Mode 1	Mode 2	Mode 3	Mode 1	Mode 2	Mode 3	Mode 1	Mode 2	Mode 3
Cantilever									
p-FEM (6)	3.30	20.82	59.52	3.52	22.16	63.35	3.30	20.82	59.52
CFEM (6)	3.31	20.88	70.61	3.52	22.22	75.16	3.31	20.88	70.61
p-FEM (10)	3.30	20.70	57.97	3.52	22.03	61.70	3.30	20.70	57.97
CFEM (10)	3.30	20.73	58.41	3.52	22.06	62.18	3.30	20.73	58.41
Yang et al.	3.30	20.70	57.97	3.52	22.03	61.70	3.30	20.70	57.97
Clamped–clamped									
p-FEM (8)	21.02	57.97	119.91	22.37	61.69	127.63	21.02	57.97	119.91
CFEM (8)	21.11	59.10	137.46	22.46	62.90	146.30	21.11	59.10	137.46
p-FEM (12)	21.02	57.94	113.59	22.37	61.67	120.90	21.02	57.94	113.59
CFEM (12)	21.03	58.17	115.16	22.39	61.92	122.58	21.03	58.17	115.16
Yang et al.	21.02	57.94	113.59	22.37	61.67	120.90	21.02	57.94	113.59

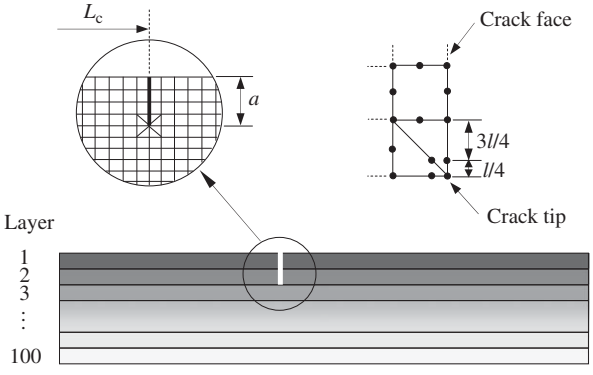

Fig. 3. The multilayer plate model of FGM beams and illustration of the finite element mesh at the cracked region.

normalized by $\bar{\omega} = \omega/\sqrt{D_0/I_0}$, where D_0 and I_0 are the corresponding values of D_{11} and I_1 of an isotropic homogeneous beam ($E_2/E_1 = 1$), are listed in Table 1, where numbers in parentheses denote the number of system dof used. The non-dimensional natural frequencies of FGM beams with $E_2/E_1 = 0.2$ and 5.0 are the same because the values of D_{11}/I_1 are identical. Table 1 presents that with the same dof, the results obtained by the *p*-FEM converge more rapidly to Yang's solutions than those by the CFEM.

In the following validation examples, two-dimensional FEM of the FGM beam with a crack are established using the commercial FE package ANSYS. The FGM beam is firstly assumed to consist of 100 layers of uniform height containing isotropic homogeneous materials, as shown in Fig. 3. The material parameters are constant in each layer and the average of the values on the top and the bottom surface of the corresponding layer. The reason of making such assumption lies in two facts: (1) the FGM beam can be modeled as a multilayer plate structure when sufficient layers are adopted [37] and (2) the stresses around the crack tip have conventional square-root singularity if the material properties are continuous or piecewise differentiable [33]. Then the multilayer plate structure is discretized using the 8-node quadrilateral plane stress element PLANE42, which has two dof at each node, namely, the displacements in the nodal x and y directions. The edge crack is modeled by generating two independent sets of nodes along the crack surfaces. The quadrilateral elements around the crack tip are reduced to be triangular-shaped. In addition, the mid-side nodes of these

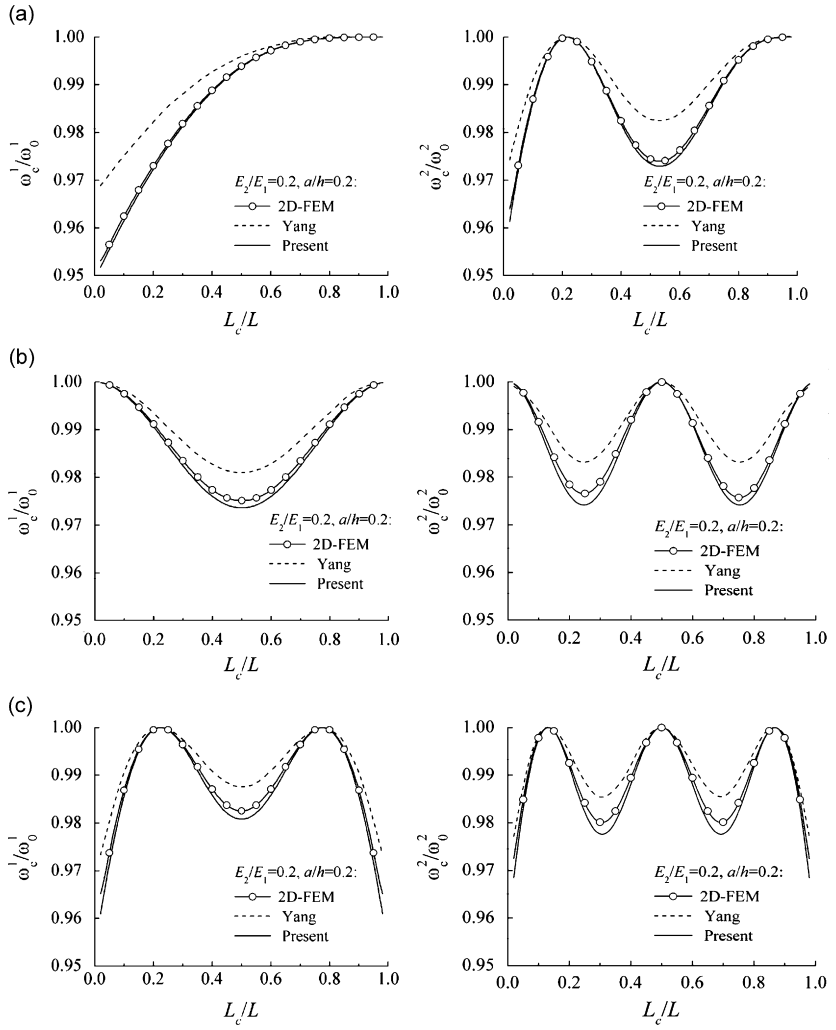

Fig. 4. The first two frequency ratios of FGM beams with an edge crack at varying locations for different boundary conditions: (a) cantilever, (b) hinged–hinged and (c) clamped–clamped.

triangular elements are moved to 1/4 point of the corresponding side in order to produce the required stress singularity, as illustrated in Fig. 3.

The above two-dimensional finite element models are used to analyze the vibration characteristics of FGM beams with cantilever, hinged–hinged and clamped–clamped supporting conditions. Also, the present *p*-FEM using 8 terms of shape functions is applied to solve the corresponding one-dimensional problems. The ratios of the first two natural frequencies of the cracked cantilever, hinged–hinged, clamped–clamped FGM beams to those of the intact counterparts are plotted in Fig. 4, obtained by the above methods and given by Yang et al. [26]. It can be seen that the results by the present method are more close to the two-dimensional models analysis compared with Yang's results. It should be noted that the derivation of the local flexibility by Yang et al. is based on the original analytical SIF solution, i.e. Eq. (14). The fundamental frequency ratios of cantilever FGM beams with an edge crack for different material gradients $E_2/E_1 = 1$ and 5, are shown in Fig. 5. Excellent agreement of the proposed method with the two-dimensional FEM analysis is again observed, while the approach by Yang et al. produces large errors in such cases. From the above examples, the efficiency and accuracy of the present crack modeling and the proposed *p*-FEM formulation are demonstrated.

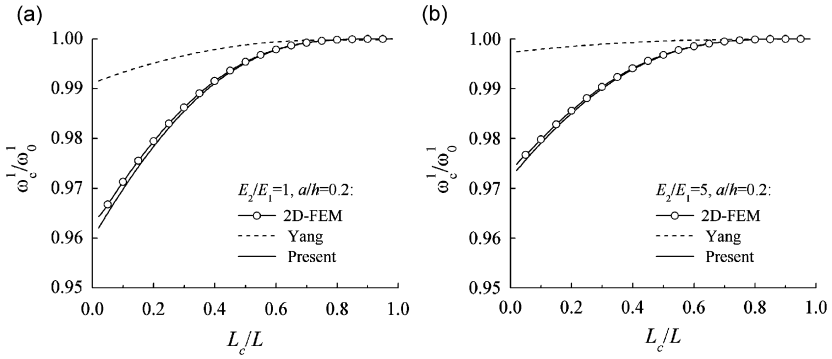

Fig. 5. Fundamental frequency ratio of cantilever FGM beams with an edge crack for different material gradients: (a) $E_2/E_1 = 1$ and (b) $E_2/E_1 = 5$.

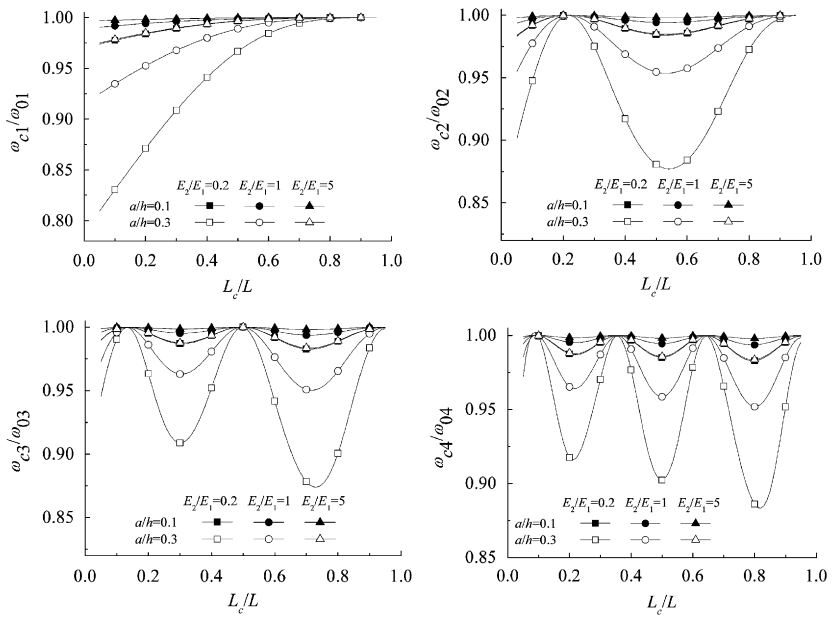

Fig. 6. The first four natural frequency ratios of a cantilever FGM versus crack location for different crack sizes and material gradients.

4. Vibration analysis of cracked FGM beams

After testing the proposed p-FEM formulation, vibration analysis of a cracked cantilever FGM beam of slenderness ratio $L/h = 20$ is carried out and discussed below. In the present calculation, 8 terms of shape functions are also employed to approximate the transverse displacement fields within the two p-version FGM beam elements used. Dynamic behavior of FGM beams with other supporting conditions can be investigated in the similar means.

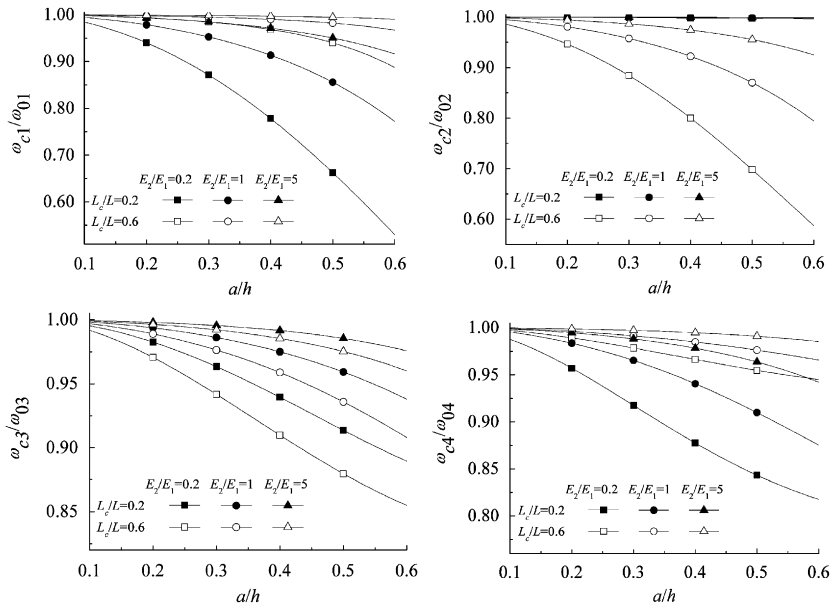

Fig. 7. The first four natural frequency ratios of a cantilever FGM beam versus crack size for different crack locations and material gradients.

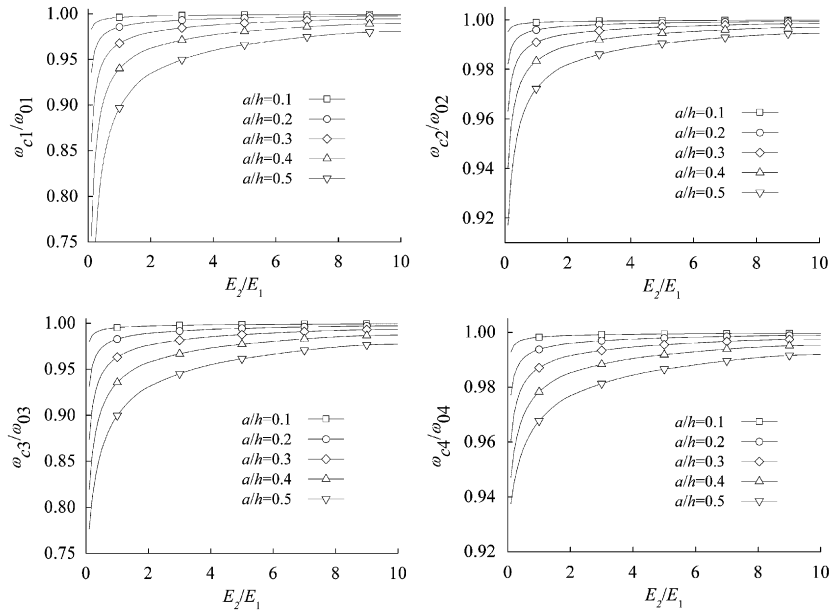

Fig. 8. The first four natural frequency ratios of a cantilever FGM beam versus material gradient ($L_c/L = 0.3$).

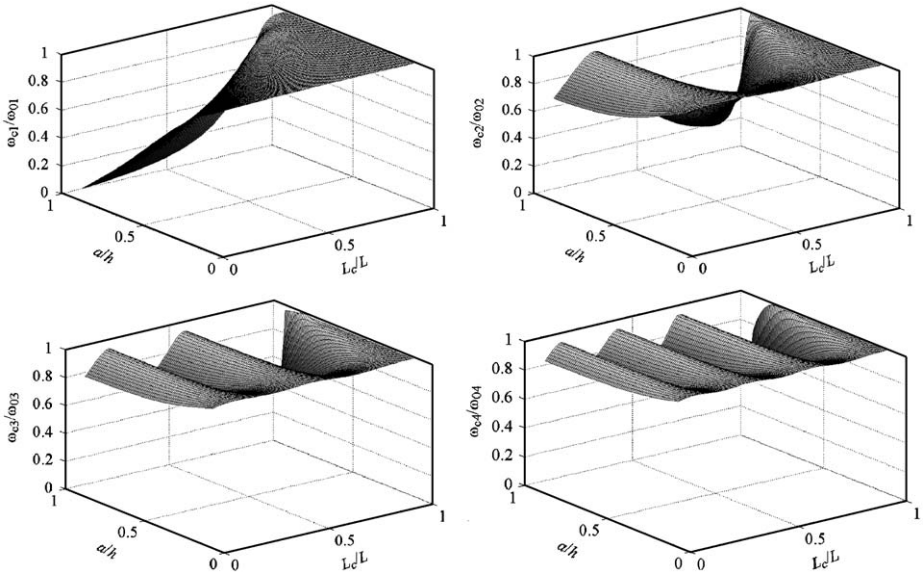

Fig. 9. The first four natural frequency ratio versus crack size and location for a cantilever FGM beam.

Fig. 6 shows the first four natural frequency ratios as functions of crack location for different normalized crack sizes and material gradients. It can be seen that the first four natural frequency ratios vary with the normalized crack location. For a specific normalized crack size and material gradient, the crack at the fixed end has a most severe effect on the reduction of the fundamental frequency. Additionally, a fact that may be derived from the figure is that when the crack located at certain positions, the natural frequencies of the second mode or the higher modes keep unchanged. These positions are usually called vibration nodes for a given mode.

The first four natural frequency ratios as functions of crack depth for different crack locations and material gradients are shown in Fig. 7. As indicated from the figure, the first four natural frequency ratios vary with the normalized crack size. For a certain normalized crack location and material gradient, the first four frequency ratios would monotonically decrease as the crack size increases. It can be derived from the fact the crack would introduce local flexibility and then lead to loss of structural stiffness.

The first four natural frequency ratios as functions of material gradients for some crack sizes and a certain crack location ($L_c/L = 0.3$) are given in Fig. 8. It can be found that the natural frequencies of each mode are more severely affected when the elastic gradient E_2/E_1 is much less than 1 and vice versa. As the elastic gradient increases, the rate of increase of each modal frequency gradually decreases. This phenomenon is due to that the value of the material gradient determines whether the crack is located on the compliant or the stiff side of the FGM beam.

A three-dimensional plot of the natural frequency ratio versus normalized crack location and size is shown in Fig. 9. From the above analysis, it could be deduced that the natural frequencies are influenced by both the crack location and crack size of the cracked FGM beam and the extent of influence would vary depending on the material gradient.

5. Crack identification by frequency contours

As shown above, both crack location and size have influence on the frequencies of the cracked FGM beam for a certain material gradient. It indicates that one frequency could be related to different crack locations and sizes. Based on this understanding, the contour curve, which has the same frequency ratio corresponding to different combinations of crack locations and sizes, could be plotted in a figure with normalized crack locations and sizes as its axes. Fig. 10 shows frequency ratio contours for the first four modes of a cantilever FGM beam with slenderness ratio $L/h = 20$ and material gradient $E_2/E_1 = 0.2$ containing an open edge crack,

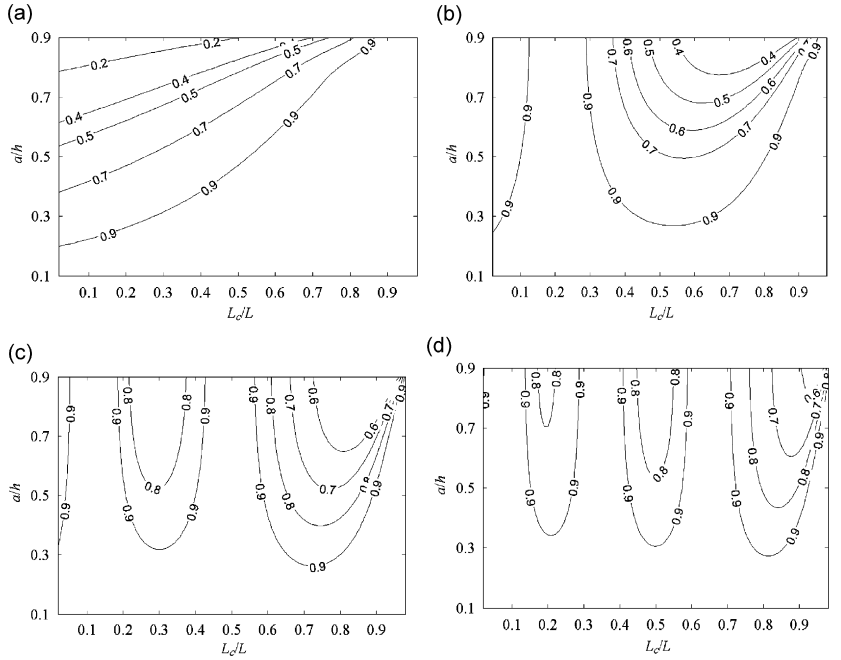

Fig. 10. Frequency ratio contours for a FGM cantilever beam with an edge crack: (a) mode 1, (b) mode 2, (c) mode 3 and (d) mode 4.

Table 2
Crack cases and prediction results for different error levels.

Crack case	Reference crack		Error rate	Predicted crack		Prediction error	
	L_c/L	a/h	(%)	L_c/L	a/h	Location (%)	Size (%)
1	0.2	0.2	1	0.197	0.204	1.5	2.0
			2	0.186	0.232	7.1	15.8
2	0.2	0.4	1	0.198	0.405	1.0	1.3
			2	0.193	0.424	3.5	6.0
3	0.4	0.2	1	0.404	0.186	1.0	7.0
			2	0.407	0.174	1.8	13.0
4	0.4	0.4	1	0.398	0.406	0.5	1.5
			2	0.401	0.395	0.3	1.3
5	0.6	0.2	1	0.582	0.211	3.0	5.5
			2	0.571	0.224	4.8	12.0
6	0.6	0.4	1	0.595	0.404	0.8	1.0
			2	0.598	0.388	0.3	3.0

which are obtained by the proposed *p*-FEM. The location and size corresponding to any point on the curve would become the possible crack location and size. Although two reference frequency ratios are theoretically sufficient to identify the crack in the beam, two frequency ratio contour lines may intersect at more than one point. Therefore, three reference frequency ratios are usually required to uniquely determine the two unknown crack parameters.

In the present study, the reference frequency ratios as inputs to the frequency contours are taken as

$$\left(\frac{\omega_{cj}}{\omega_{0j}}\right)^{*} = \left(\frac{\omega_{cj}}{\omega_{0j}}\right)^{c} + err \cdot \varepsilon_j, \quad j = 1, 2, 3, \tag{20}$$

where $(\omega_{cj}/\omega_{0j})^{c}$ are the calculated frequency ratios with a prescribed scenario of the crack, *err* represents the modeling and measurement error rate, ε is a number random from uniform distribution in the interval $[-0.5$

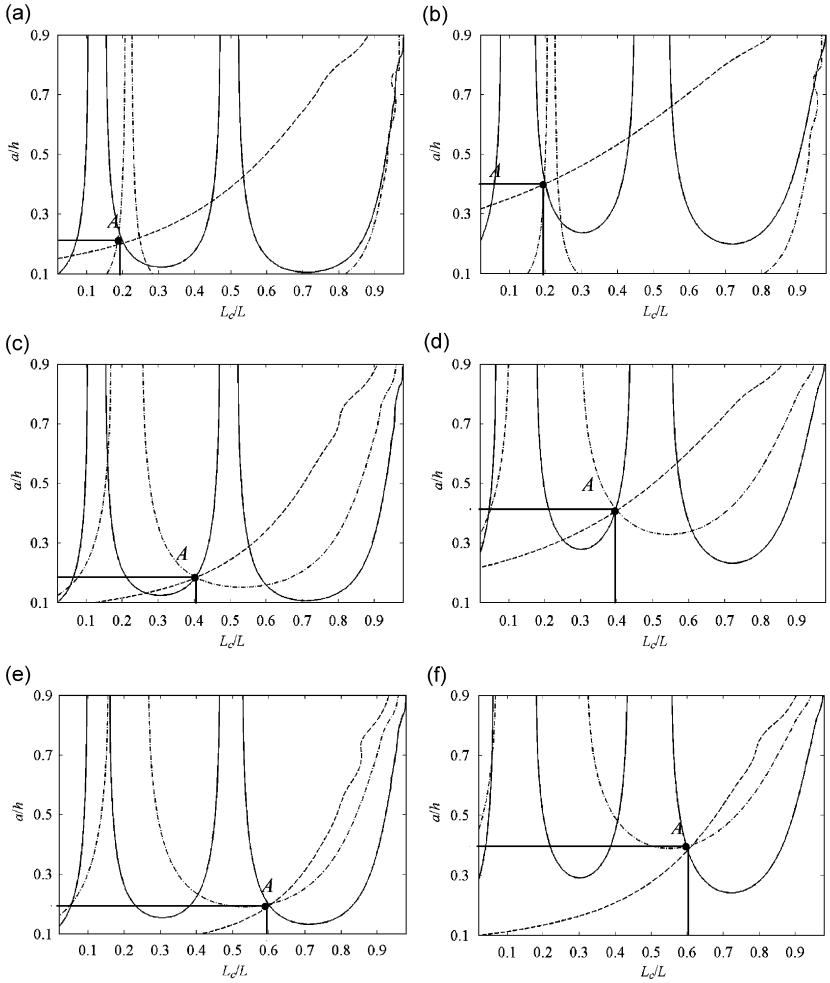

Fig. 11. Crack identification by frequency contour from the first three modes (- - - mode 1, - · - mode 2, — mode 3): (a) case 1, (b) case 2, (c) case 3, (d) case 4, (e) case 5 and (f) case 6.

0.5]. Here *err* is taken as 1% and 2% and six scenarios of the crack are considered, as listed in Table 2. Then the reference frequency ratios generated from Eq. (20) are employed as inputs to acquire the frequency contours for each mode. In the presence of the measurement and modeling error, the three contour curves do not intersect at one point. In this situation, the centroid of the three pairs of intersections is taken as the crack location and size. The crack locations and sizes obtained from 20 simulations for each crack scenario are averaged to get their mean values. Fig. 11 shows the crack identification results by using the frequency contour plots with $err = 2\%$ in one sample for illustrative purpose. The intersection A of the three curves indicates the crack location and size. Table 2 presents the comparison of the reference crack parameters and the predicted crack parameters for different error rates in various scenarios. Several things can be observed from this table. First, the precision of crack parameter identification generally gets worse as the measurement and modeling error increases. Second, the crack size has been detected with less accuracy than the crack location. Third, the identification errors decrease as the crack size becomes larger.

6. Conclusions

A methodology based on the *p*-FEM to detect crack location and size is developed in this paper. Because of the favorable features of the *p*-FEM, the present formulation is a useful tool to deal with high-performance

computation in structural crack identification of FGM beams. A rational approximation of SIF with material gradient and crack size as two independent variables is presented in order to facilitate crack modeling in FGM beams. Subsequently the crack is represented by a massless rotational spring and its stiffness can be computed from fracture mechanics. The accuracy and convergence of the proposed *p*-version finite element formulation and the crack modeling are validated by the literature results for intact FGM beams and two-dimensional analysis for cracked FGM beams, respectively. It should be noted that the present crack modeling based on the rational approximation algorithm along with the *p*-FEM formulation may be extended to simulate in a very concise and efficient way the effect of cracks for which the SIF of FGM with arbitrary material property distributions were obtained by theoretical or numerical approaches. The effects of crack size and location and material gradient on the natural frequencies of cracked cantilever FGM beams are investigated in detail. The frequency contours for various modes with respect to crack location and size are plotted together and the intersection of these contours could point out the predicted crack location and size. Numerical experiments have demonstrated that the present method has excellent computational efficiency compared with the CFEM and satisfactory identification performance even with simulated measurement and modeling errors. As mentioned before, FGM have found increasingly attractive applications in space structures, fusion reactors and so on. Therefore, the dynamics and diagnosis of cracked FGM beams investigated in this paper is of practical significance and able to be used in structural health monitoring.

Acknowledgments

This work was supported by the Natural Science Foundation of China for Distinguished Young Scholars (no. 50425516), the Natural Science Foundation of China (Key Program) (no. 10732060) and the National High Technology Research and Development Program of China (863 Program) (no. 2006AA04Z438). Comments and suggestions from the anonymous referees as well as helpful advices by Dr. Z.K. Peng and Dr. J.S. Zhao are sincerely appreciated.

References

[1] A.O. Ayhan, Stress intensity factors for three-dimensional cracks in functionally graded materials using enriched finite elements, *International Journal of Solids and Structures* 44 (2007) 8579–8599.
[2] P. Gu, R.J. Asaro, Cracks in functionally graded materials, *International Journal of Solids and Structures* 34 (1997) 1–17.
[3] Z. Cheng, Z. Zhong, Fracture analysis of a functionally graded strip under plane deformation, *Acta Mechanica Solida Sinica* 19 (2006).
[4] F. Erdogan, B.H. Wu, The surface crack problem for a plate with functionally graded properties, *Journal of Applied Mechanics* 64 (1997) 449–456.
[5] T.G. Chondros, A.D. Dimarogonas, Dynamic sensitivity of structures to cracks, *Journal of Vibration, Acoustics, Stress and Reliability in Design* 111 (1989) 251–256.
[6] A.D. Dimarogonas, Vibration of cracked structures: a state of the art review, *Engineering Fracture Mechanics* 55 (1996) 831–857.
[7] O.S. Salawu, Detection of structural damage through changes in frequency: a review, *Engineering Structures* 19 (1997) 718–723.
[8] S.W. Doebling, C.R. Farrar, M.B. Prime, D.W. Shevitz, A review of damage identification methods that examine changes in dynamic properties, *Shock and Vibration Digest* 30 (1998) 91–105.
[9] T.G. Chondros, A.D. Dimarogonas, J. Yao, Vibration of a beam with a breathing crack, *Journal of Sound and Vibration* 239 (1) (2001) 57–67.
[10] P.F. Rizos, N. Aspragathos, A.D. Dimarogonas, Identification of crack location and magnitude of a cantilever beam from the vibration mode, *Journal of Sound and Vibration* 138 (1990) 381–388.
[11] Y. Narkis, Identification of crack location in vibrating simply supported beams, *Journal of Sound and Vibration* 172 (4) (1994) 549–558.
[12] M.H. Dado, A comprehensive crack identification algorithm for beams under different end conditions, *Applied Acoustics* 51 (4) (1997) 381–398.
[13] S. Christides, A.D.S. Barr, One-dimensional theory of cracked Bernoulli–Euler beams, *International Journal of Mechanical Sciences* 26 (1984) 639–648.
[14] T.G. Chondros, The continuous crack flexibility model for crack identification, *Fatigue and Fracture of Engineering Materials and Structures* 24 (10) (2001) 643–650.
[15] X.F. Yang, A.S.J. Swamidas, R. Seshadri, Crack identification in vibrating beams using the energy method, *Journal of Sound and Vibration* 244 (2) (2001) 339–357.

[16] M. Karthikeyan, R. Tiwari, S. Talukdar, Crack localisation and sizing in a beam based on the free and forced response measurements, *Mechanical Systems and Signal Processing* 21 (2007) 1362–1385.
[17] M.W. Suh, M.B. Shim, M.Y. Kim, Crack identification using hybrid neuro-genetic technique, *Journal of Sound and Vibration* 238 (4) (2000) 617–635.
[18] F.T.K. Au, Y.S. Cheng, L.G. Tham, Z.Z. Bai, Structural damage detection based on a micro-genetic algorithm using incomplete and noisy modal test data, *Journal of Sound and Vibration* 259 (5) (2003) 1081–1094.
[19] G.M. Owolabi, A.S.J. Swamidas, R. Seshadri, Crack detection in beams using changes in frequencies and amplitudes of frequency response functions, *Journal of Sound and Vibration* 265 (2003) 1–22.
[20] G.D. Gounaris, C.A. Papadopoulos, Crack identification in rotating shafts by coupled response measurements, *Engineering Fracture Mechanics* 69 (3) (2002) 339–352.
[21] J. Woo, S.A. Meguid, L.S. Ong, Nonlinear free vibration behavior of functionally graded plates, *Journal of Sound and Vibration* 289 (2006) 595–611.
[22] E. Efraim, M. Eisenberger, Exact vibration analysis of variable thickness thick annular isotropic and FGM plates, *Journal of Sound and Vibration* 299 (2007) 720–738.
[23] C.M.C. Roque, A.J.M. Ferreira, R.M.N. Jorge, A radial basis function approach for the free vibration analysis of functionally graded plates using a refined theory, *Journal of Sound and Vibration* 300 (2007) 1048–1070.
[24] M. Aydogdu, V. Taskin, Free vibration analysis of functionally graded beams with simply supported edges, *Materials & Design* 28 (2007) 1651–1656.
[25] L.W. Byrd, V. Birman, Vibrations of damaged functionally graded cantilever beams, *Multiscale and Functionally Graded Materials Conference 2006* (*M&FGM2006*), Honolulu, 2006.
[26] J. Yang, Y. Chen, Free vibration and buckling analyses of functionally graded beams with edge cracks, *Composite Structures* 83 (2008) 48–60.
[27] J. Yang, Y. Chen, Y. Xiang, X.L. Jia, Free and forced vibration of cracked inhomogeneous beams under an axial force and a moving load, *Journal of Sound and Vibration* 312 (2008) 166–181.
[28] E. Viola, L. Federici, L. Nobile, Detection of crack location using cracked beam element method for structural analysis, *Theoretical and Applied Fracture Mechanics* 36 (2001) 23–35.
[29] D.Y. Zheng, N.J. Kessissoglou, Free vibration analysis of a cracked beam by finite element method, *Journal of Sound and Vibration* 273 (2004) 457–475.
[30] M. Kisa, J. Brandon, M. Topcu, Free vibration analysis of cracked beams by a combination of finite elements and component mode synthesis methods, *Computers & Structures* 67 (1998) 215–223.
[31] B. Szabo, I. Babuska, *Finite Element Analysis*, Wiley, New York, 1991.
[32] F. Delale, F. Erdogan, The crack problem for a nonhomogenous plane, *Journal of Applied Mechanics* 50 (1983) 609–614.
[33] N. Noda, Z.H. Jin, Thermal stress intensity factors for a crack in a strip of a FGM, *International Journal of Solids and Structures* 30 (8) (1993) 1039–1056.
[34] G.C. Sih, Strain energy density factor applied to mixed mode problems, *Engineering Fracture Mechanics* 10 (1974) 305–321.
[35] H. Tada, P.C. Paris, G.R. Irwin, *The Stress Analysis of Cracks Handbook*, third ed., ASME Press, New York, 2000.
[36] T. Mura, T. Koya, *Variational Methods in Mechanics*, Oxford University Press, New York, 1992.
[37] B.L. Wang, Y.W. Mai, N. Noda, Fracture mechanics analysis model for functionally graded materials with arbitrarily distributed properties, *International Journal of Fracture* 116 (2002) 161–177.